

Phase Structure of Hot and/or Dense QCD in the Schwinger-Dyson Approach

Satoshi TAKAGI

Department of Physics, Nagoya University, Nagoya 464-8602, Japan

We investigate the phase structure of hot and/or dense QCD with massless 2-flavors using the Schwinger-Dyson equation (SDE) with the improved ladder approximation in the Landau gauge. We examine the effect of the antiquark contribution and find that setting the antiquark Majorana mass equal to the quark one is a good approximation in the medium density region. The imaginary part of the Dirac mass has an important influence on the chiral phase transition, in particular on the tricritical point.

§1. Introduction

The exploration of the QCD phase diagram, including the color superconducting phase, is an important subject for the purpose of studying not only the dynamics of QCD but also its phenomenological applications in cosmology, the astrophysics of neutron stars and the physics of heavy ion collisions.¹⁾ The phase structure of QCD at non-zero temperature (T) with zero chemical potential has been extensively studied with lattice simulations, but the simulations at finite chemical potential (μ) has begun only recently and these simulations still involve large errors [see, e.g., Refs. 2) and references cited therein]. Thus, it is important to investigate the phase structure of QCD in the finite T and/or μ region by many other approaches.

In various non-perturbative approaches, the approach based on the Schwinger-Dyson Equation (SDE) is one of the most powerful tools [see references cited in Ref. 3)]. From the SDE with a suitable running coupling, the high energy behavior of the mass function is shown to be consistent with the result derived from QCD with the operator product expansion and the renormalization group equation. Furthermore, the SDE include the effect of the long range force mediated by the magnetic mode of the gluon, which may have a substantial effect, even in the intermediate chemical potential region, as in the high density region.⁴⁾⁻⁷⁾ In the SDE analysis, the phase structure of QCD in the finite T and/or μ region have been investigated, concentrating on the chiral symmetry restoration.⁸⁾⁻¹¹⁾

In Ref. 3) we solved the coupled SDE for the Majorana masses of the quark (Δ^-) and antiquark (Δ^+) separately from the SDE for the Dirac mass (B) in the low and intermediate temperature and chemical potential region. The true vacuum is determined by comparing the values of the effective potential at these solutions. Here we report the results in Ref. 3) and add a figure in order to emphasize the effect of the imaginary part of the Dirac mass.

§2. Phase structure

The phase diagram obtained in Ref. 3) is shown in Fig. 1. We consider the possibility of three phases: the hadron phase, the two-flavor color superconducting (2SC) phase^{12),13)} and the quark-gluon plasma (QGP) phase. The value of the pion decay constant f_π is 88 MeV. There are two notable features in Fig. 1. One is the position of the tricritical point: $(T, \mu) = (146, 20)$ MeV (indicated by \square in Fig. 1). The origin of this feature in the SDE is discussed in the next section. The

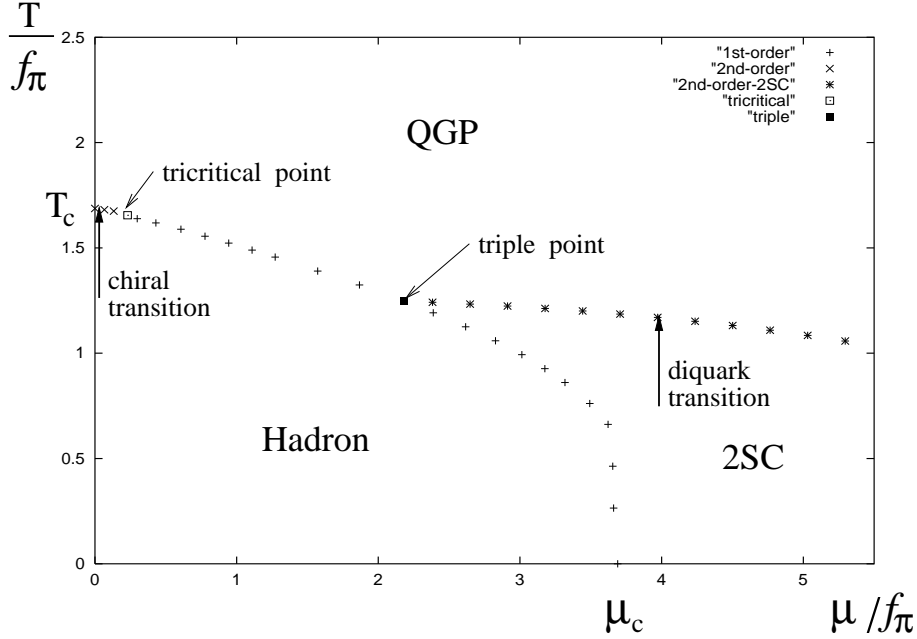


Fig. 1. Phase diagram for $0 \leq T/f_\pi \leq 2.5$ and $0 \leq \mu/f_\pi \leq 5.5$. The symbol \times denotes the second order phase transition between the hadron phase and the QGP phase, $+$ the first order phase transition between the hadron phase and the QGP phase or the 2SC phase, and $*$ the second order phase transition between the 2SC phase and the QGP phase. $T_c=147$ MeV, $\mu_c=325$ MeV, and $(T, \mu)=(146, 20)$ MeV at the tricritical point, where the second order phase transition changes to first order. The value of the pion decay constant f_π is 88 MeV.

other is the high critical temperature of the color phase transition ($2SC \leftrightarrow QGP$). It is around 100 MeV for any μ satisfying $\mu \lesssim 500$ MeV, and this value is larger than those obtained in models based on the contact 4-Fermi interaction[see, e.g., Ref. 14)]. This increase of the critical temperature may be caused by the long range force.

We examined the antiquark contribution of the 2SC phase in Ref. 3). Our results show that the antiquark Majorana mass gap, Δ^+ , is comparable to the quark one, Δ^- , in all the chemical potential regions that we studied: $1 > \Delta^+/\Delta^- \gtrsim 0.85$ for $0 < \mu \lesssim 500$ MeV.³⁾ However, we find that Δ^+ can not be generated in the SDE without Δ^- .³⁾ Therefore the anti-quark gap Δ^+ is generated radiatively by the quark gap Δ^- as shown in the weak coupling limit.¹⁵⁾

§3. Effect of the imaginary part of the Dirac mass

The value of μ at the tricritical point (end point) obtained in Fig. 1 is much smaller than those in several other models, such as the 4-Fermi interaction model^{14),16)} as well as in the other SDE analysis,^{10),11)} but is consistent with that obtained in Ref. 9), which was also obtained through the analysis of the SDE. We find that in the framework of the SDE, the large difference in the position of the tricritical point in the T - μ plane is caused by the existence of the imaginary part of the Dirac mass B at $\mu \neq 0$.³⁾ See Fig. 2, in which the chiral phase transition points are shown for two cases: one is the SDE analysis with $\text{Im}[B] \neq 0$ and the other is that with $\text{Im}[B] = 0$. When we use the SDE without the imaginary part of the Dirac mass (i.e., $\text{Im}[B] = 0$), the tricritical point is at $(T, \mu) = (124, 210)\text{MeV}$. The value of μ at this tricritical point [$\mu \sim O(100)\text{MeV}$] is close to the values obtained from analyses carried out using models with the local 4-Fermi interaction^{14),16)} and those carried out using the SDEs without $\text{Im}[B]$.^{10),11)}

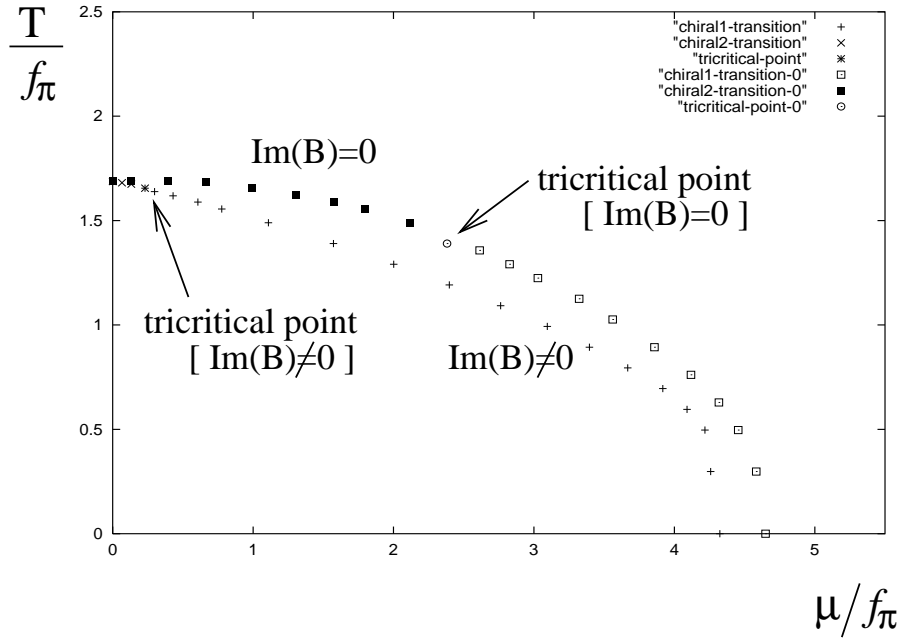


Fig. 2. Phase diagrams in two different cases for $0 \leq T/f_\pi \leq 2.5$ and $0 \leq \mu/f_\pi \leq 5.5$. The 2SC phase is not considered for simplicity. The lower- T points show the chiral phase transition points obtained from the SDE with $\text{Im}[B]$, while the higher- T points show those obtained from the SDE without $\text{Im}[B]$. f_π is 88 MeV.

In Ref. 3) we performed analysis with the imaginary part of the Dirac mass included, because in the SDE at non-zero chemical potential, the imaginary part $\text{Im}[B]$, is inevitably generated in the hadron phase.^{3),17)} However, some analyses of the SDE do not include the imaginary part,^{10),11)} and analyses done using the local 4-Fermi interaction model do not generally include the imaginary part, because a leading order approximation is used.

§4. Summary and discussion

We studied the phase structure of hot and/or dense QCD (with massless 2 flavors) by solving the Schwinger-Dyson equations for the Dirac and Majorana masses of the quark propagator with the improved ladder approximation in the Landau gauge. There are two notable features: One is the position of the tricritical point ($\mu \sim 20\text{MeV}$) and the other is the rather large critical temperature ($T \sim 100\text{MeV}$) at the color phase transition. We find that the antiquark mass is of the same order as the quark mass in the low and medium density region, and setting $\Delta^+ = \Delta^-$ is actually a good approximation for investigating the phase diagram, the quark Majorana mass gap and the diquark condensate.

We emphasize the importance of the imaginary part of the Dirac mass at nonzero chemical potential. We perform the analysis with the imaginary part of the Dirac mass $\text{Im}[B]$ included, because the imaginary part is inevitably generated in the chiral symmetry breaking phase in the SDE at non-zero μ . We find that the most noteworthy feature of the analysis that includes the imaginary part of the Dirac mass is in the position of the tricritical point on the T - μ plane. In the SDE analysis, including the imaginary part causes the tricritical point to move to a position of much smaller μ : $(T, \mu) = (124, 210)\text{MeV} \rightarrow (T, \mu) = (146, 20)\text{MeV}$.

Acknowledgements

The author would like to thank D. K. Hong for informing his work.¹⁵⁾

References

- 1) K. Rajagopal and F. Wilczek, hep-ph/0011333;
M. G. Alford, Ann. Rev. Nucl. Part. Sci. **51** (2001), 131, hep-ph/0102047.
- 2) F. Karsch and E. Laermann, hep-lat/0305025;
S. Muroya, A. Nakamura, C. Nonaka and T. Takaishi, Prog. Theor. Phys. **110** (2003), 615, hep-lat/0306031.
- 3) S. Takagi, Prog. Theor. Phys. **109** (2003), 233, hep-ph/0210227.
- 4) D. T. Son, Phys. Rev. D **59** (1999), 094019, hep-ph/9812287.
- 5) D. K. Hong, V. A. Miransky, I. A. Shovkovy and L. C. Wijewardhana, Phys. Rev. D **61** (2000), 056001, [ibid. D **62** (2000), 059903, Erratum], hep-ph/9906478.
- 6) T. Schäfer and F. Wilczek, Phys. Rev. D **60** (1999), 114033, hep-ph/9906512.
- 7) R. D. Pisarski and D. H. Rischke, Phys. Rev. D **61** (2000), 051501, nucl-th/9907041;
- 8) Y. Taniguchi and Y. Yoshida, Phys. Rev. D **55** (1997), 2283, hep-ph/9512375.
- 9) M. Harada and A. Shibata, Phys. Rev. D **59** (1999), 014010, hep-ph/9807408.
- 10) A. Barducci, R. Casalbuoni, S. De Curtis, R. Gatto and G. Pettini, Phys. Rev. D **41** (1990), 1610.
- 11) O. Kiriya, M. Maruyama and F. Takagi, Phys. Rev. D **62** (2000), 105008, hep-ph/0001108.
- 12) M. Alford, K. Rajagopal and F. Wilczek, Phys. Lett. B **422** (1998), 247, hep-ph/9711395.
- 13) R. Rapp, T. Schafer, E. V. Shuryak and M. Velkovsky, Phys. Rev. Lett. **81** (1998), 53, hep-ph/9711396.
- 14) J. Berges and K. Rajagopal, Nucl. Phys. B **538** (1999), 215, hep-ph/9804233.
- 15) D. K. Hong, Phys. Rev. D **62** (2000), 091501, hep-ph/0006105.
- 16) M. Asakawa and K. Yazaki, Nucl. Phys. A **504** (1989), 668,
- 17) M. Harada and S. Takagi, Prog. Theor. Phys. **107** (2002), 561, hep-ph/0108173.